LUNAR SURFACE ROUGHNESS, SHADOWING AND THERMAL EMISSION

March 8, 1967

B. G. Smith

Work performed for Manned Space Flight, National Aeronautics and Space Administration under Contract NASW-417.

TABLE OF CONTENTS

ABSTRACT

A statistical model of the moon's surface roughness is used in an attempt to explain the deviations of the observed gross infra-red thermal emissive properties of the moon from those characterizing a smooth Lambertian surface. Comparison of theory and experiment suggests that the thermal brightness variation across the full moon disc is affected by large scale relief of rms slope 10-20°. The method requires development of a self shadowing theory of random rough surfaces which may be used, in a different context, to determine local rms surface slope from the amount of shadow visible in a moon photograph. It is suggested that this technique may be particularly useful in the rapid analysis of Lunar Orbiter photography. Analysis of an earth-based photograph of a typical highland region yields 9° for the rms slope of large scale roughness. The rms slopes deduced agree with those found in radar studies of the moon.

LUNAR SURFACE ROUGHNESS, SHADOWING AND THERMAL EMISSION

INTRODUCTION

The surface of the moon is rough, both microscopically as deduced from photometric studies [Hopfield, 1966] and on the large scale as observed through telescopes, and various theoretical models have been constructed to incorporate the effect of surface roughness in the interpretation of lunar remote sensing experiments. A statistical description of the surface in terms of a density function of height deviations from a mean spherical moon has been particularly useful in an understanding of the lunar radar backscattering properties [Hagfors, 1964]. An attempt is made in this paper to extend the use of the statistical model to examine the effect of surface roughness on the overall emission of thermal radiation and the casting of shadows in sunlight.

The model describes the moon as a smooth sphere upon which are superimposed positive and negative undulations of height generated by a stationary random process. Locally the underlying surface may be considered plane, coinciding with the z=0 plane of a cartesian coordinate system. The density of surface height deviations (ξ) from the mean plane in the z direction is described by a continuous probability function $P_1(\xi)$, of zero mean, chosen to be Gaussian for computational ease, where the probability of finding a height deviation within the range $\Delta\xi$ about ξ is:

$$P_1(\xi)\,\Delta\xi = \frac{1}{(2\pi)^{1/2}\,\sigma} e^{-\xi^2/2\sigma^2} \cdot \Delta\xi \qquad (1)$$

and σ is the root mean square height deviation. The horizontal scale of the relief is contained within an autocorrelation function $\rho(r)$, defined by:

$$\rho(r) = \langle \xi(\underline{R}+\underline{r}) \cdot \xi(\underline{R}) \rangle \qquad (2)$$

where $\underline{R}$ and $\underline{r}$ are vectors lying in the mean plane and the average is taken over all $\underline{R}$. $\rho(r)$ is independent of the direction of $\underline{r}$ for an isotropic surface. Higher dimensional density functions and their appropriate correlation matrices may be derived from the autocorrelation function $\rho(r)$ [Middleton, 1960]. In particular, the joint density function of surface slopes $p\ (=\partial z/\partial x)$ and $q\ (=\partial z/\partial y)$ for the Gaussian surface described by equation 1 is:

$$P_{22}(p,q) = \frac{1}{2\pi w^2}\, e^{\left(-\frac{p^2+q^2}{2w^2}\right)} = P_2(p)\cdot P_2(q) \qquad (3)$$

where w^2, the mean square surface slope, is $[-\rho''(0)]$, the primes denoting double differentiation with respect to r.

Each infinitesimal element of the surface can absorb, reflect and emit radiation, and possibly shadow its fellows, and the behavior of the surface as a whole is the summation of elemental contributions.

SHADOWING THEORY

Geometrical self-shadowing of the surface presents the greatest analytical difficulty and will be discussed first, with an approach essentially similar to that used in a recent paper by Wagner [1966], suggested by Beckmann [1965]. The problem is the following: what is the probability $S(\xi_o, p_o, q_o, \theta)$ that a point F on a random rough surface, of given height ξ_o above the mean plane and with local slopes p_o, q_o will not lie in shadow when the surface is illuminated with a parallel beam of radiation at an angle of incidence θ to the mean plane? Figure 1 illustrates a section through the surface. The origin of coordinates is taken in the mean plane below F and the axes oriented with the incoming beam lying in the x=0 plane. Only parts of the surface in this plane to the right of F can shadow F, and $S(\xi_o, p_o, q_o, \theta)$, or $S(F,\theta)$ for short, is equivalent to the probability that no part of the surface to the right of F will intersect the ray FS. This in turn, may be written as the limit:

$$S(F,\theta) = \lim_{\tau\to\infty} S(F,\theta,\tau) \qquad (4)$$

where $S(F,\theta,\tau)$ is the probability that no part of the surface between $y=0$ and $y=\tau$ will intersect the ray FS. A differential equation for $S(F,\theta,\tau)$ may be developed thus:

$$S(F,\theta,\tau+\Delta\tau) = S(F,\theta,\tau) \cdot Q(\Delta\tau|F,\theta,\tau) \tag{5}$$

where now $Q(\Delta\tau|F,\theta,\tau)$ is the conditional probability that the surface will not intersect FS in the interval $\Delta\tau$ given that it does not in the interval τ. Turning this around and suppressing the functional dependence upon F,θ:

$$Q(\Delta\tau|F,\theta,\tau) = 1 - g(\tau)\Delta\tau \tag{6}$$

where $g(\tau)\Delta\tau$ is the conditional probability that the surface in $\Delta\tau$ will intersect the ray FS given that it does not in the interval τ. Equation 5 now becomes, again suppressing explicit F and θ dependence:

$$S(\tau+\Delta\tau) = S(\tau) \cdot \{1 - g(\tau)\Delta\tau\} \tag{7}$$

Expanding $S(\tau+\Delta\tau)$ about τ in a Taylor Series to first order in $\Delta\tau$ leads to the differential equation:

$$\frac{dS(\tau)}{d\tau} = - g(\tau) \cdot S(\tau) \tag{8}$$

which may be integrated to yield:

$$S(\tau) = S(0)\exp\left\{- \int_0^\tau g(\tau)d\tau\right\} \tag{9}$$

$S(0)$ will clearly be unity if q_o is less than cot θ and zero otherwise, so $S(0) = h(\mu - q_o)$, where h is the unit step function and $\mu = \cot \theta$. Equation 4 now becomes:

$$S(F,\theta) = h(\mu - q_o)\exp\left\{-\int_0^\infty g(\tau)d\tau\right\} \tag{10}$$

The heart of the task lies in the evaluation of $g(\tau)$ and the subsequent integration over τ. Instead of an attempt at a complete analysis $g(\tau)$ will be approximated by replacing $g(\tau)\Delta\tau$ with the conditional probability that F will be shadowed by the surface in $\Delta\tau$ given that it is not shadowed by the surface at $y=\tau$. (This avoids the difficulty of including the effects of correlation between points on the surface in $\Delta\tau$ and the infinity of points in τ.)

If the surface at τ does not shadow F,

$$\xi(\tau) < \xi_o + \mu\tau \tag{11}$$

symbolically denoted as circumstance α.

If the surface in $\Delta\tau$ does shadow F, and $q \equiv q(\tau)$,

$$\xi(\tau) < \xi_o + \mu\tau \; ; \quad \xi(\tau+\Delta\tau) > \xi_o + \mu(\tau+\Delta\tau) \; ; \quad q \geq \mu \tag{12}$$

that is: $\xi(\tau)$ must lie in the interval $(q-\mu)\Delta\tau$ below $\xi_o + \mu\tau$, and $q \geq \mu$, denoted as circumstance β. $g(\tau)\Delta\tau$ is just the conditional probability that β will occur given α, or:

$$g(\tau)\Delta\tau = P(\beta|\alpha) \tag{13}$$

A well known relationship in probability theory links $P(\beta|\alpha)$ with $P(\alpha,\beta)$ and $P(\alpha)$, respectively, the probability of α and β occurring independently and the probability of α occurring by itself:

$$P(\alpha,\beta) = P(\beta|\alpha) \cdot P(\alpha) \tag{14}$$

therefore,

$$g(\tau)\Delta\tau = \frac{P(\alpha,\beta)}{P(\alpha)} \tag{15}$$

If $P_3(\xi,q|F,\tau)$ is the joint probability density function of ξ and q at $y=\tau$ conditional upon given height and slopes at F, then from the meaning of circumstances α and β, equations 11 and 12,

$$P(\alpha,\beta) = \Delta\tau \int_{\mu}^{\infty} dq\ (q-\mu) \left[P_3(\xi,q|F,\tau)\right]_{\xi = \xi_o + \mu\tau} \tag{16}$$

and

$$P(\alpha) = \int_{-\infty}^{+\infty} dq \int_{-\infty}^{\xi_o+\mu\tau} d\xi\ P_3(\xi,q|F,\tau) \tag{17}$$

and so

$$g(\tau)\Delta\tau = \frac{\Delta\tau \int_{\mu}^{\infty} dq(q-\mu) \left[P_3(\xi,q|F,\tau)\right]_{\xi=\xi_o+\mu\tau}}{\int_{-\infty}^{+\infty} dq \int_{-\infty}^{\xi_0+\mu\tau} d\xi\ P_3(\xi,q|F,\tau)} \tag{18}$$

where the renormalization effected by the denominator allows for the condition that $\xi(\tau)$ is known to be $\leq \xi_o + \mu\tau$.

With known distribution and autocorrelation functions the integrals in equation 18 may be evaluated in full, but this is a tedious process and not illuminating. Great simplicity is gained by neglecting correlation between the height and slopes at F and those at $y=\tau$. The conditional density function in this case reduces to a product of simple Gaussian functions:

$$P_3(\xi,q|F,\tau) = P_1(\xi)P_2(q) = \frac{1}{2\pi\sigma w} e^{-\xi^2/2\sigma^2 - q^2/2w^2} \quad (19)$$

and within this approximation equation 18 becomes:

$$g(\tau) = \frac{\mu(2\pi)^{1/2}\ \Lambda(\mu) \cdot e^{-\frac{(\xi_o+\mu\tau)^2}{2\sigma^2}}}{\sigma\left[2 - \mathrm{erfc}\left(\frac{\xi_o+\mu\tau}{\sqrt{2}\sigma}\right)\right]} \quad (20)$$

where erfc is the error function complement and:

$$2\Lambda(\mu) = \left(\left(\frac{2}{\pi}\right)^{1/2} \cdot \frac{w}{\mu} e^{-\mu^2/2w^2} - \mathrm{erfc}(\mu/\sqrt{2}w)\right) \quad (21)$$

The integration over τ (equation 10) is now simple and leads to:

$$S(F,\theta) = S(\xi_o,p_o,q_o,\theta) = h(\mu-q_o)\left[1 - 1/2\ \mathrm{erfc}(\xi_o/\sqrt{2}\sigma)\right]^{\Lambda} \quad (22)$$

Two further distributions may be deduced from $S(F,\theta)$: the probability of F not being shadowed, independent of ξ_o, which is:

$$S(p_o,q_o,\theta) = \int_{-\infty}^{+\infty} S(\xi_o,p_o,q_o,\theta)\, P_1(\xi_o)\, d\xi_o = \frac{h(\mu-q_o)}{[\Lambda(\mu)+1]} \quad (23)$$

and the probability that a point on the surface will not be shadowed, independent of height and slope, $S(\theta)$:

$$S(\theta) = \int_{-\infty}^{+\infty} d\xi_o \int_{-\infty}^{+\infty} dp_o \int_{-\infty}^{+\infty} dq_o P_1(\xi_o) P_2(p_o) P_2(q_o) S(\xi_o,p_o,q_o,\theta)$$

$$= \frac{[1 - 1/2\ \mathrm{erfc}(\mu/\sqrt{2}w)]}{[\Lambda(\mu) + 1]} \quad (24)$$

The expression for $S(\theta)$ is compared in Figure 2 with that derived by Brockelman and Hagfors [1966] from a computer simulation of an illuminated Gaussian random rough surface; good agreement is achieved between present theory and 'experiment'. Wagner [1966] does not use the device of renormalization, equation 18, and instead includes correlation directly in the form of a Gaussian autocorrelation function to evaluate the conditional probability function $P_3(\xi,q|F,\tau)$. He is forced to approximate the integral over τ, equation 10, and at the expense of analytical complexity in fact gains a closer agreement with the simulation. Equation 24 provides an adequate approximation for the present purpose, and as will be seen later contains an advantage in satisfying a self-consistency condition. Recalling the salient result of shadowing theory which will be needed subsequently: the probability that a point on the surface with local slopes p,q will be illuminated by a beam of incidence angle θ is:

$$S(p,q,\theta) = \frac{h(\mu - q)}{[\Lambda(\mu) + 1]} = S(q,\theta) \text{ (independent of p)} \quad (25)$$

where the subscripts have been dropped from p and q.

OPTICAL SHADOWING

A measurement of the fraction of a rough surface visibly illuminated yields $S(\theta)$ directly and would provide an experimental means of investigating the statistical parameters of the surface; in the case of a Gaussian surface it would allow a determination of the rms slope. To explain the method shadowing theory must be developed further. Figure 3a illustrates a section of a rough surface illuminated from the right. δA is a surface element at F with local normal FN; FV is normal to the mean plane and FS is the illuminating ray. FK is the direction to a distant observer, and for simplicity it will be assumed that FK lies in the plane of illumination, defined as that plane containing FV and FS. The visibly illuminated area of the whole surface projected onto the plane perpendicular to the direction of view is:

$$\iint_{\text{surface}} dA\ J(p,q,\theta,\phi)\ \cos\hat{KFN} = \iint_{\substack{\text{mean}\\ \text{plane}}} dxdy\ J(p,q,\theta,\phi)\ \frac{\cos\hat{KFN}}{\cos\hat{VFN}} \tag{26}$$

where p,q are the local slopes at F and where J is a function having the value unity if δA can be seen to be illuminated and zero otherwise. Integration over a large area A_o in the mean plane is equivalent to taking an average over the distribution of illuminated facets (invoking the ergodic theorem) and so:

$$\begin{aligned}\text{projected illuminated area} &= A_o \int_{-\infty}^{+\infty} dp \int_{-\infty}^{+\infty} dq\ P_2(p)P_2(q)T(p,q,\theta,\phi)\ \frac{\cos\hat{KFN}}{\cos\hat{VFN}} \\ &= fA_o \cos\phi \end{aligned} \tag{27}$$

where f is the fraction of the total projected area illuminated and $T(p,q,\theta,\phi)$ is the probability that a point with slopes p,q

will not be shadowed for either of the ray directions FS or FK. It is necessary to consider three distinct ranges of ϕ, and the sign convention will be used in which angles measured toward the source of illumination are to be positive.

(a) $\underline{\phi > \theta}$

The joint probability T may be decomposed into the product of a conditional and a joint probability:

$$T(p,q,\theta,\phi) = \bar{T}(p,q,\theta|\phi)\ T'(p,q,\phi) \tag{28}$$

where $\bar{T}(p,q,\theta,|\phi)$ is the probability that the surface does not obstruct the ray FS given that it does not obstruct FK, and $T'(p,q,\phi)$ is the probability that the surface does not obstruct FK. $\bar{T}$ is necessarily equal to unity if $\phi > \theta$, and T' simply $S(q,\phi)$; thus:

$$T(p,q,\theta,\phi) = S(q,\phi) = h(\bar{\mu} - q)\ G(\bar{\mu}) \tag{29}$$

where

$$\bar{\mu} = \cot\ \phi \text{ and } G(\bar{\mu}) = \frac{1}{[\Lambda(\bar{\mu}) + 1]}$$

(b) $\underline{0 < \phi < \theta}$

An argument exactly parallel to (a) in which the roles of θ and ϕ are interchanged leads to:

$$T(p,q,\theta,\phi) = S(q,\theta) = h(\mu - q)\ G(\mu) \tag{30}$$

where, as before, $\mu = \cot\ \theta$.

(c) $\phi < 0$

In this case it may be assumed to a good approximation that the shadowing functions for θ and ϕ are independent, then T decomposes into the product:

$$T(p,q,\theta,\phi) = S(q,\theta) \cdot S(q,\phi)$$

$$= h(\mu-q)\ h(\bar{\mu}+q)\ G(\mu)\ G(\bar{\mu}) \qquad (31)$$

Using (a), (b) or (c) the integral in equation 27 may be evaluated and for cases (b) and (c) it yields:

(b) $$f = S(\theta) \cdot \{1 - \mu/\bar{\mu}\} + \mu/\bar{\mu} \qquad (32)$$

or

$$\frac{(f - \mu/\bar{\mu})}{(1 - \mu/\bar{\mu})} = S(\theta) \qquad (33)$$

(c)

$$f = S(\theta)\cdot G(\bar{\mu})\cdot\{1+\mu/\bar{\mu}\} + G(\mu)\cdot\{1-G(\bar{\mu})\}$$

$$- (\mu/\bar{\mu})\cdot G(\bar{\mu}) \qquad (34)$$

If the observer views the surface away from grazing angle, ($\bar{\mu} \gtrsim w$), $G(\bar{\mu})$ is close to unity and equation 34 becomes:

$$f = S(\theta)\cdot\{1 + \mu/\bar{\mu}\} - \mu/\bar{\mu} \qquad (35)$$

(a result of similar form to equation 32 which could equally well have been deduced by replacing $S(q,\phi)$ by unity in the expression for $T(p,q,\theta,\phi)$, equation 31), and:

$$S(\theta) = \frac{(f + \mu/\bar{\mu})}{(1 + \mu/\bar{\mu})} \tag{36}$$

where the sign change reflects the sense of the angle of observation. If, as well, $f\bar{\mu} >> \mu$, i.e., $|\phi| << \theta$, both expressions reduce to the simple form

$$f \simeq S(\theta) \tag{37}$$

If $\theta=\phi$, then equation 32 reduces to f=1, demonstrating that:

$$\iint_{\text{surface}} dA\ J(p,q,\theta,\theta)\ \cos\ \hat{KFN} = A_0\ \cos\ \theta \tag{38}$$

which expresses the selfconsistency condition mentioned earlier, that the visible area of a rough surface projected onto the plane perpendicular to the direction of view is independent of the roughness and equal to the projected area of the underlying mean plane, as indeed it must be. Here lies the advantage of equation 25 over the equivalent expression of Wagner [1966]. With the form of $S(q,\theta)$ derived in this paper equation 38 is satisfied identically, not approximately. The selfconsistency condition also ensures that f=1 for $\phi>\theta$, (case (a)).

The condition imposed upon the orientation of the direction of view in the plane of illumination may be relaxed at the cost of greater care in the analysis of the joint probability function $T(p,q,\theta,\phi)$. Here attention will be restricted to the regime where equations 33 and 36 are valid. On the moon this limits observation to the equatorial region and a measurement of the shadows cast in sunlight allows, within the model,

a direct determination of the rms slope of local surface roughness on the scale of resolution of the photographs used. $S(\theta)$ calculated according to equations 33 and 36 from measurements of the proportion of area shadowed in atlas photographs [Kopal, 1965] of a highland area north of Julius Caesar crater [15°E, 5°N], is displayed in Figure 4, with theoretical curves calculated for various values of the rms slope w. Statistical uniformity of the surface across the region examined ($\sim$ 180 x 180 km^2) was assumed and the effect of varying sun angle deduced from different north-south strips of the same photograph. Included in the diagram is a point taken from a shadow analysis in a highland region near the crater Argelander [5°E, 15°S] made in a different connection by Watson, et al [1961]. Comparison with theory suggests an rms slope of $\sim$ 9°, which if typical of large parts of the moon compares well with the value of $\sim$ 10° deduced from radar studies [Evans and Hagfors, 1966] for structure of greater than meter scale.

While of interest in connection with earth-based lunar photographic studies it is suggested that shadow analysis may be useful also in estimating meter scale surface roughness from high resolution Lunar Orbiter photography which would provide a means for the rapid screening of photographs during the process of selection of a site for an Apollo landing.

INFRA-RED EMISSION STUDIES

Observers of the infra-red emission of the moon have noticed two phenomena which are conventionally attributed to surface roughness. Pettit and Nicholson [1930] and, more recently, Ingrao, Young and Linsky [1966] observed the change of infra-red brightness across the equatorial belt of the full moon disc and found that the brightness decreased more slowly than the cosine of the angle of observation which would be expected for a spherical Lambertian surface. Sinton [1962] who measured the brightness of the subsolar point over a lunation noticed an angular dependence of the brightness not given by a spherical Lambertian surface. An attempt will be made to interpret both these observations in terms of surface roughness of a scale below the resolution of the detector.

Each surface element of the rough moon is assumed to be a perfect Lambertian emitter of thermal radiation at the wavelengths concerned. Heat flow through the surface is neglected (a good approximation during the lunar day) and energy balance for the surface element used to equate absorbed sunlight with radiated thermal energy. The contribution to the radiation incident on an element emitted or reflected by its

fellows is neglected, as is any angular dependence of the absorption coefficient. Emissive and absorptive properties are assumed uniform across the surface, a section of which is illustrated in Figure 3b illuminated from vertically above and observed at a distance from the direction FK. The total energy absorbed and hence radiated by the element δA is proportional to $\delta A \cos \hat{VFN}$, and that reaching the observer proportional to:

$$\delta A \cos \hat{VFN} \cos \hat{NFK} \left[J(p,q,\theta,\phi)\right]_{\theta=0} \tag{39}$$

The total radiation, E, reaching the observer from the surface is:

$$E \propto \iint_{\substack{\text{mean} \\ \text{plane}}} dxdy \cos \hat{NFK}\, J(p,q,0,\phi) \tag{40}$$

Averaging over the surface, dividing by the projected area and normalizing gives the observed brightness, $B_A(\phi)$,

$$B_A(\phi) = \frac{B_A(0)}{I} \int_{-\infty}^{+\infty} \int_{-\infty}^{+\infty} dpdq\, P_2(p) \cdot P_2(q)\, \frac{[1-q \tan \phi]}{(1+p^2+q^2)^{1/2}}\, S(q,\phi) \tag{41}$$

where

$$\cos \hat{VFN} = \frac{1}{(1 + p^2 + q^2)^{1/2}}$$

$$\cos \hat{NFK} = \frac{\cos \phi - q \sin \phi}{(1 + p^2 + q^2)^{1/2}}$$

and

$$I = \int_{-\infty}^{+\infty} dp \int_{-\infty}^{+\infty} dq \; P_2(p) \; P_2(q) \; \frac{1}{[1+p^2+q^2]^{1/2}} \quad (42)$$

$B_A(\phi)$ calculated numerically from equation 41 for various values of surface rms slope w is shown as a function of ϕ in Figure 5, upon which are superimposed the experimental findings of Sinton [1962] for the brightness of the subsolar point.

The change of brightness across the full moon disc requires slightly different analysis. In Figure 3c an element of the surface is illustrated, illuminated and observed from the same angle ϕ. Arguments similar to those preceding equation 40 lead to an expression for the radiated energy reaching the observer from the whole surface:

$$E \propto \iint_{\substack{\text{mean} \\ \text{plane}}} dxdy \; \frac{\cos^2 \hat{NFK}}{\cos \hat{VFN}} \; J(p,q,\phi,\phi) \quad (43)$$

The apparent brightness of the surface as a function of the angle of incidence is just:

$$B_B(\phi) = \frac{B_B(0) \cos \phi}{I}$$

$$\cdot \int_{-\infty}^{+\infty} \int_{-\infty}^{+\infty} dpdq \; P_2(p) \; P_2(q) \; \frac{[1-q \tan \phi]^2}{(1+p^2+q^2)^{1/2}} \; S(q,\phi) \quad (44)$$

Values of $B_B(\phi)$ computed from equation 44 are displayed in Figure 6, compared with the experimental observations of Ingrao, et al [1966].

In each case it is seen that theory explains the qualitative features of the observations. The limbs of the full moon disc are brighter than expected for a smooth sphere, because the collection of randomly oriented facets provides an array radiating in the direction of the observer more efficiently than the equivalent smooth surface. Conversely the subsolar point is less bright than expected, for an analogous reason.

Both $B_A(\phi)$ and $B_B(\phi)$ approach limits as $\phi \to \pi/2$:

$$B_A(\pi/2) = B_A(0) \frac{(2\pi)^{1/2}}{Iw} \int_{-\infty}^{+\infty} dp \int_0^{\infty} dq \; P_2(p) \; P_2(q) \frac{q}{[1+p^2+q^2]^{1/2}} \tag{45}$$

and

$$\lim_{w \to 0} B_A(\pi/2) = B_A(0) \tag{46}$$

$$B_B(\pi/2) = B_B(0) \frac{(2\pi)^{1/2}}{Iw} \int_{-\infty}^{+\infty} dp \int_0^{\infty} dq \; P_2(p) \; P_2(q) \frac{q^2}{[1+p^2+q^2]^{1/2}} \tag{47}$$

and

$$\lim_{w \to 0} B_B\left(\frac{\pi}{2}\right) \sim \left[B_B(0) \cdot \left(\frac{\pi}{2}\right)^{1/2} \cdot w\right] \to 0 \tag{48}$$

Quantitative agreement of theory and experiment is satisfactory in one case but less so in the other. If the model can be trusted it appears that infra-red thermal brightness across the full moon disc is affected primarily by the large scale structure of rms slope 10-20°. The model correctly predicts that the brightness should not fall to zero at the

limb, a feature of the experimental results. Agreement with the measurements of Sinton [1962] is quantitatively poor, but to approach them it seems necessary to invoke a high degree of roughness, small scale structure with 60-70° rms slope, to explain the marked darkening of the subsolar point at the limb. It is not obvious why there should be this discrepancy.

The possibility of the presence of extreme roughness suggests that to describe the physical situation more closely the model should be improved to include the illumination of a facet by radiation reflected and emitted by those adjacent; as Sinton [1962] has pointed out the 'valleys' will then be hotter than the 'peaks' and the apparent brightness dependent upon the proportion of each visible. In addition, a complete theory should take account of the whole range of roughness in a coherent way rather than divide structure into two classes, the one of microscopic scale responsible for producing the Lambertian behavior assumed to be characteristic of the other coarser relief, a separation made implicitly in this paper.

B G Smith

1014-BGS-jdc B. G. Smith

REFERENCES

Beckmann, P., Shadowing of random rough surfaces, IEE Trans. on Antennas and Propagation, Ap 13, 384-388, 1965.

Brockelman, R. A., and T. Hagfors, Note on the effect of shadowing on the backscattering of waves from a random rough surface, IEE Trans. on Antennas and Propagation, AP 14, 621-626, 1966.

Evans, J. V., and T. Hagfors, Study of radio echoes from the moon at 23 centimeters wavelength, J. Geophys. Res., 71 (20), 4871-4889, 1966.

Hagfors, T., Backscattering from an undulating surface with applications to radar returns from the moon, J. Geophys. Res., 69 (18), 3779-3784, 1964.

Hopfield, J. J., Mechanism of lunar polarization, Science, 151, 1380-1381, 1966.

Ingrao, H. C., A. T. Young, and J. L. Linsky, A critical analysis of lunar temperature measurements in the infrared, Chapter 10 in The Nature of the Lunar Surface, Proceedings of the 1965 IAU-NASA Symposium, edited by W. N. Hess, D. H. Menzel and J. A. O'Keefe, The Johns Hopkins Press, Baltimore, 1966.

Kopal, Z., plates XXXVIII and CXV of Photographic Atlas of the Moon, Academic Press Inc., New York, 1965.

Middleton, D., Chapters 7 and 8 in Introduction to Statistical Communication Theory, McGraw-Hill Book Co., Inc., New York, 1960.

Pettit, E., and S. B. Nicholson, Lunar radiation and temperatures, Astrophys. J., 71, 102-135, 1930.

Sinton, W. M., Temperatures on the lunar surface, in Physics and Astronomy of the Moon, edited by Z. Kopal, Academic Press Inc., New York, 1962.

Wagner, R. J., Shadowing of randomly rough surface, T. R. W. Systems Report 7401-6012-R0000, 1966.

References (continued)

Watson, K., B. C. Murray, and H. Brown, The behavior of volatiles on the lunar surface, J. Geophys. Res., 66 (9), 3033-3045, 1961.

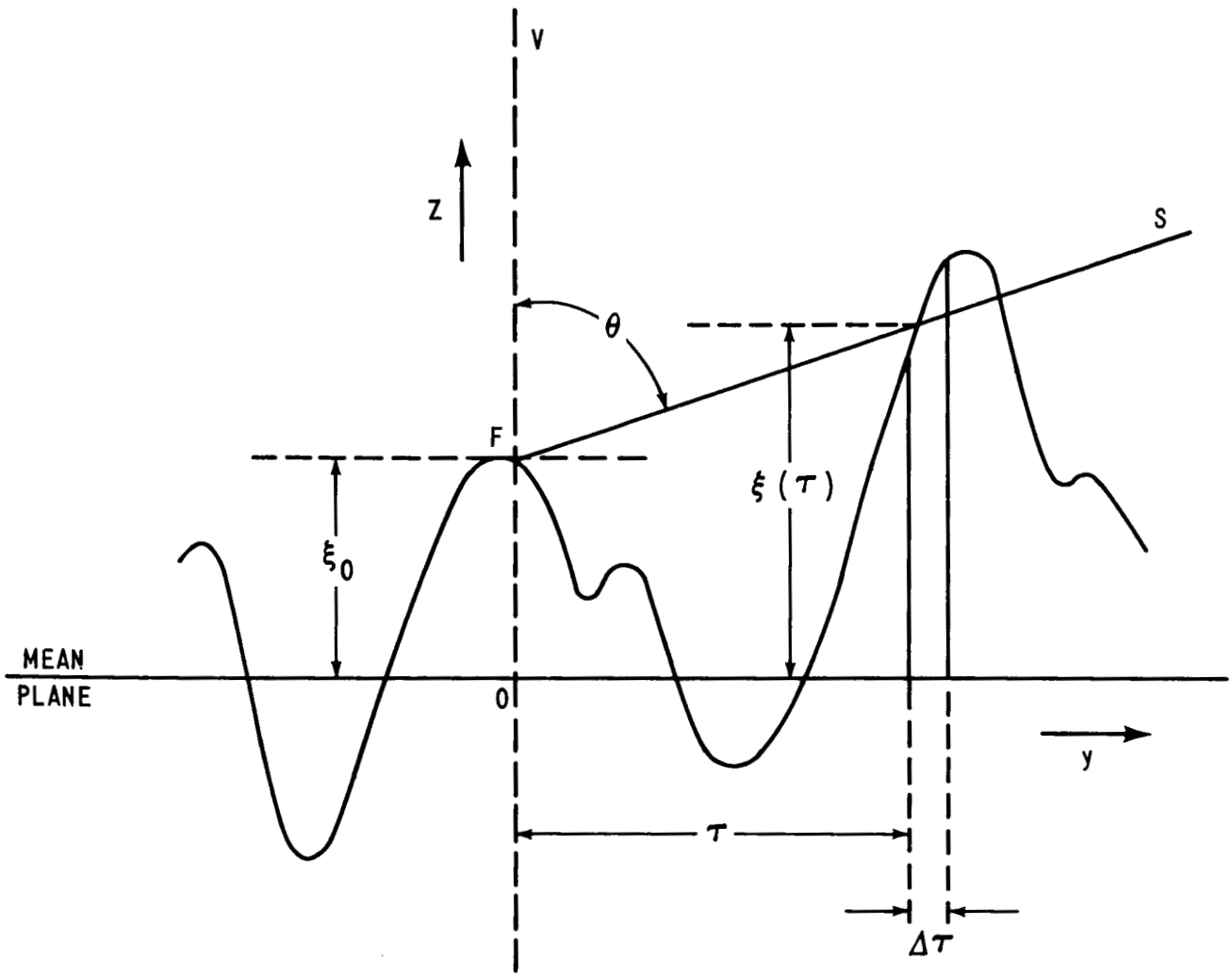

FIGURE I SECTION OF A RANDOM ROUGH SURFACE ILLUMINATED FROM S.

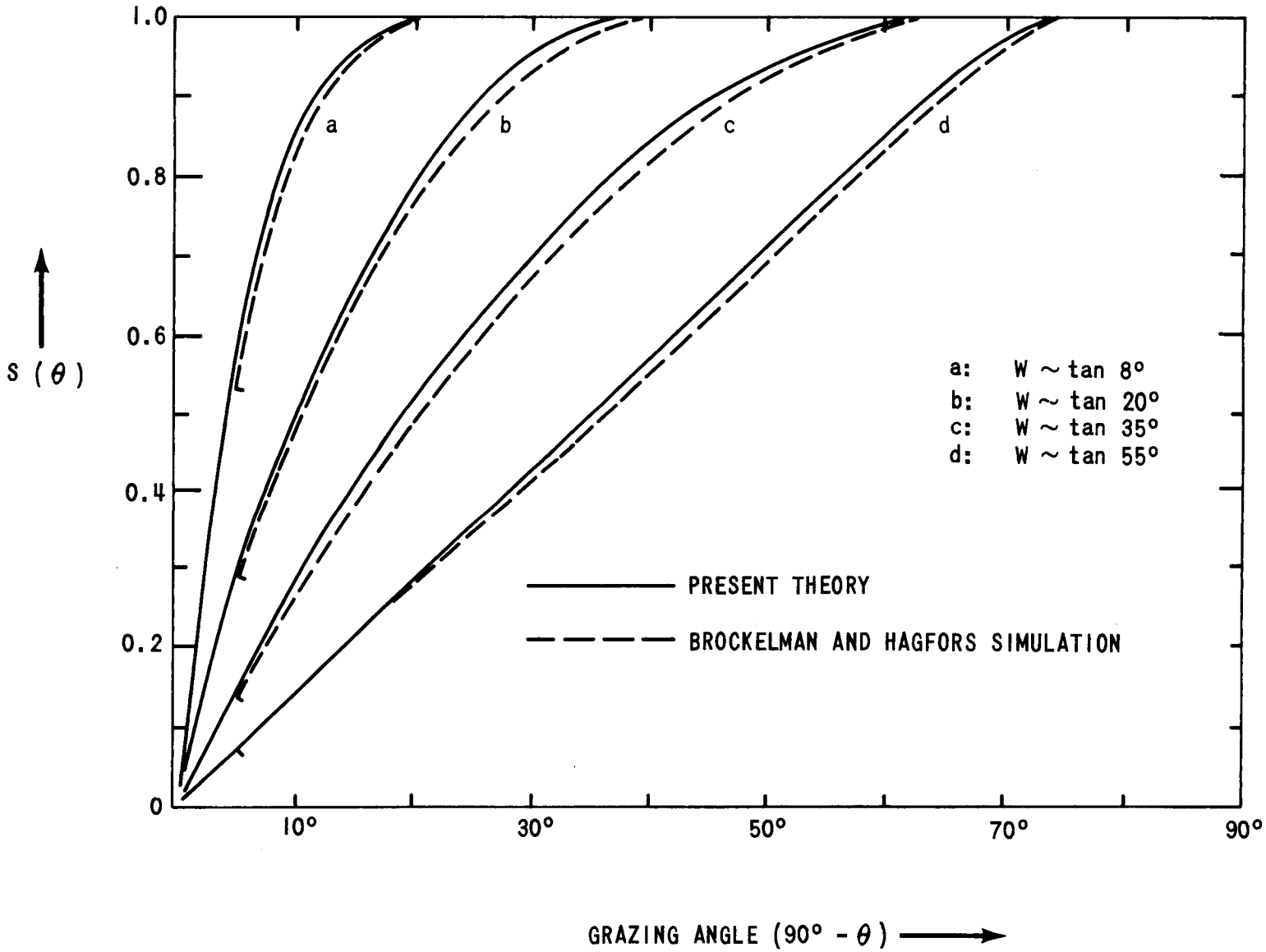

FIGURE 2 COMPARISON OF THE THEORETICAL SHADOWING FUNCTION $S(\theta)$ WITH THE SIMULATION OF BROCKELMAN AND HAGFORS (1966).

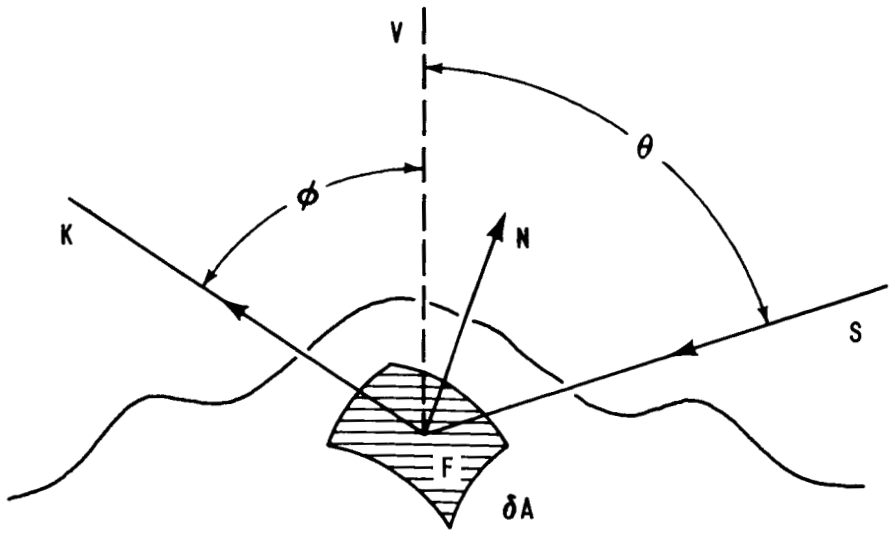

FIGURE 3a PART OF A RANDOM ROUGH SURFACE ILLUMINATED FROM S AND OBSERVED FROM K.

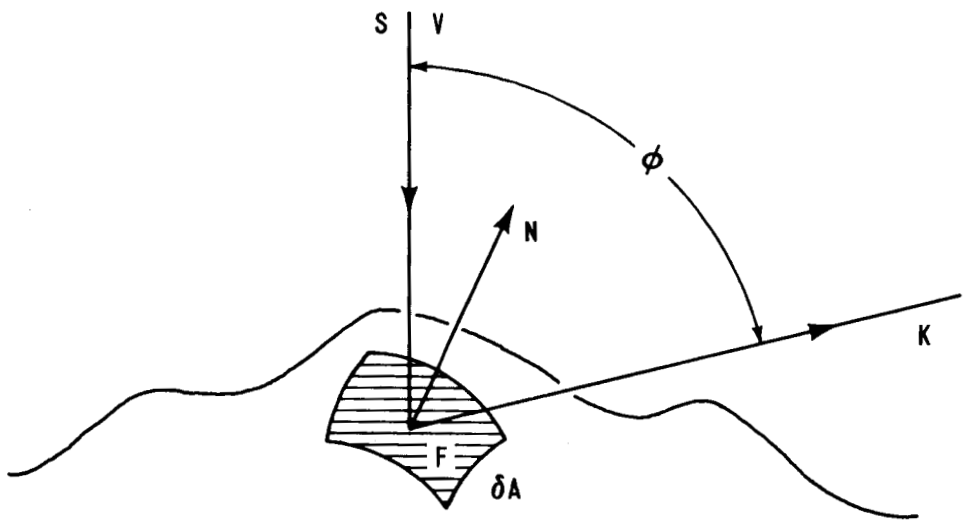

FIGURE 3b PART OF A RANDOM ROUGH SURFACE ILLUMINATED FROM VERTICALLY ABOVE AND OBSERVED FROM K.

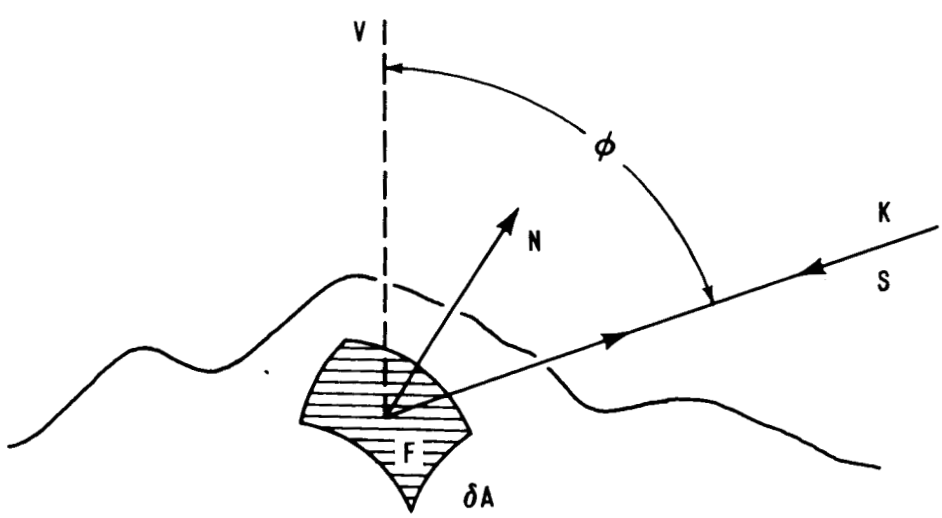

FIGURE 3c PART OF A RANDOM ROUGH SURFACE BOTH ILLUMINATED AND OBSERVED FROM K.

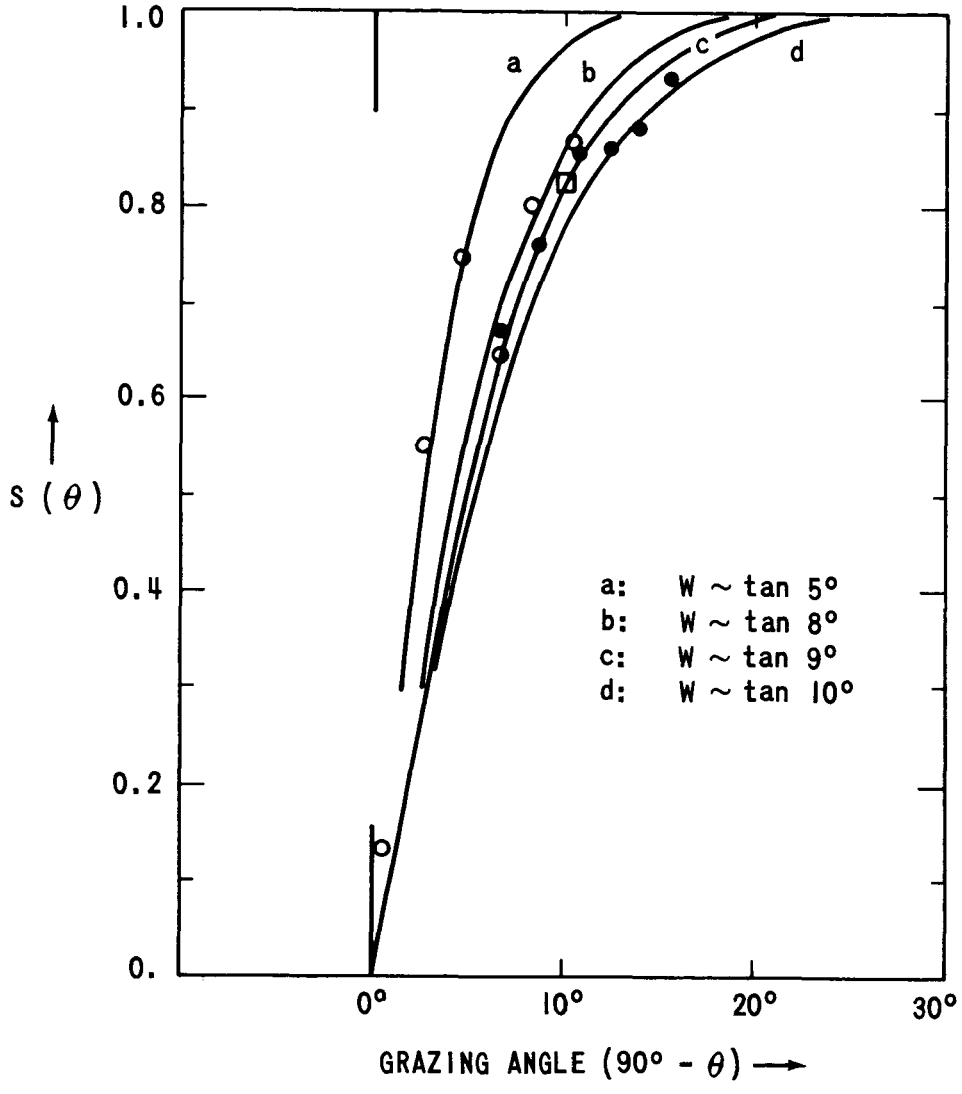

○ : HIGHLAND AREA NEAR JULIUS CAESAR CRATER (SUNRISE)

● : HIGHLAND AREA NEAR JULIUS CAESAR CRATER (SUNSET)

□ : HIGHLAND AREA NEAR ARGELANDER CRATER

FIGURE 4 SHADOWING FUNCTION S(θ) MEASURED FROM MOON PHOTOGRAPHS COMPARED WITH THEORETICAL CURVES.

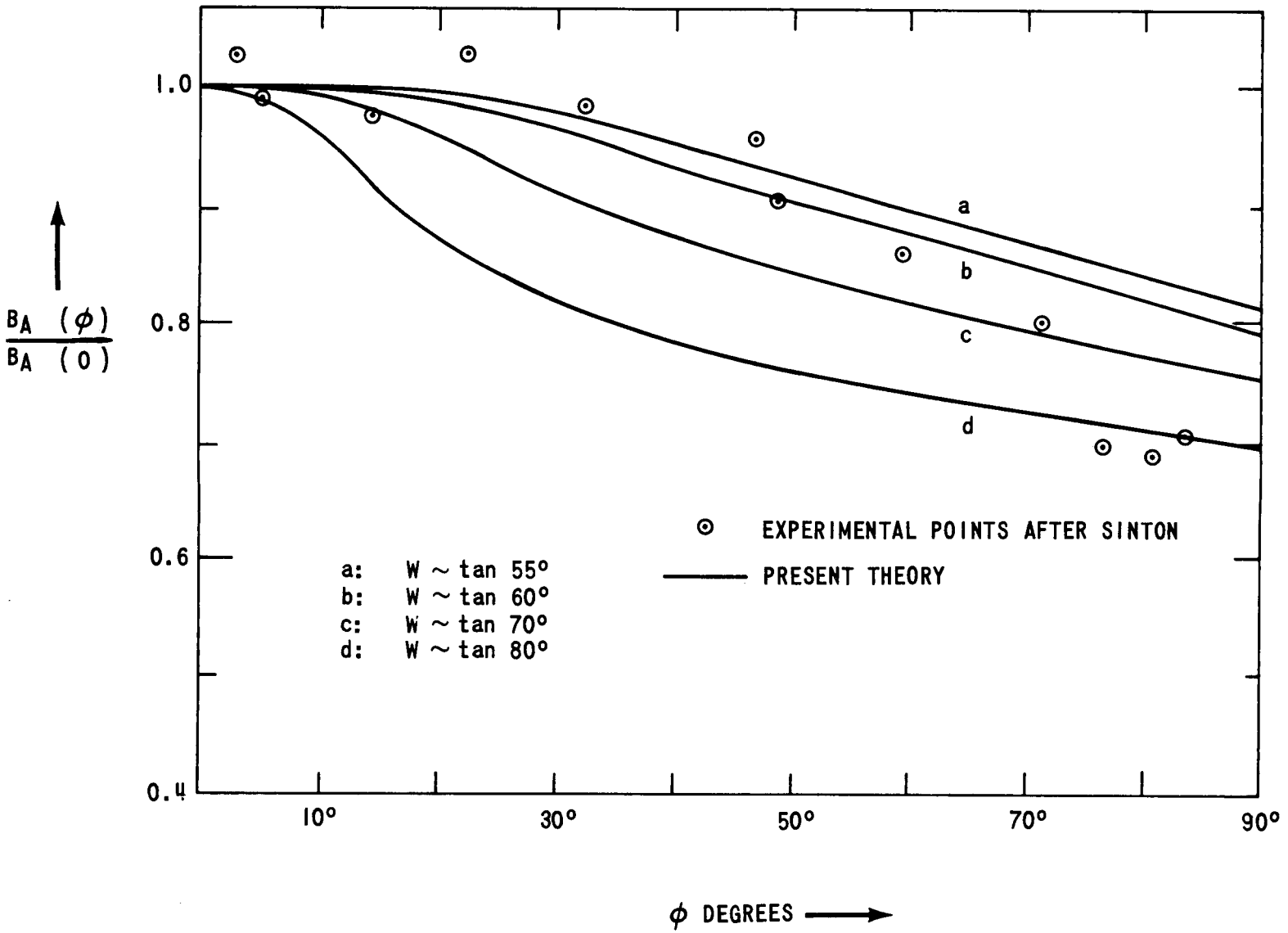

FIGURE 5 INFRA-RED BRIGHTNESS VARIATION OF THE SUBSOLAR POINT DURING A LUNATION (AFTER SINTON (1962)) COMPARED WITH THEORETICAL CURVES.

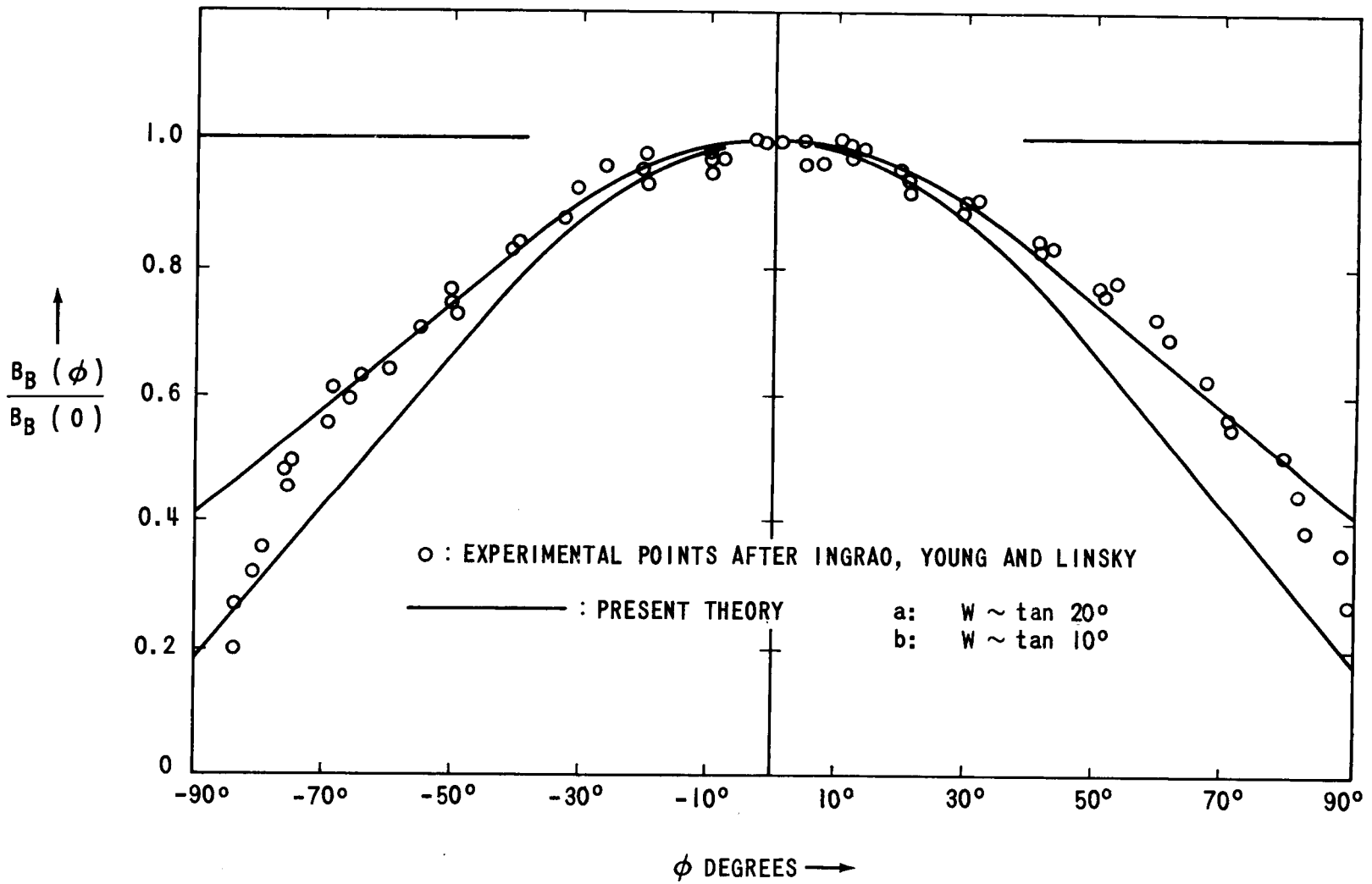

FIGURE 6 INFRA-RED BRIGHTNESS VARIATION ACROSS THE FULL MOON DISC (AFTER INGRAO, YOUNG AND LINSKY (1966)) COMPARED WITH THEORETICAL CURVES.

DISTRIBUTION LIST

NASA Headquarters

W. C. Beckwith - MTP
P. E. Culbertson - MTL
E. M. Davin - SL
L. E. Day - MAT
F. P. Dixon - MTY
S. E. Dwornik - MTY
E. Z. Gray - MT
E. W. Hall - MTS
J. K. Holcomb - MAO
T. A. Keegan - MA-2 (6)
D. R. Lord - MTD
S. C. Phillips - MA
M. J. Raffensperger - MTE
L. Reiffel - MA-6
L. R. Scherer - SL
A. D. Schnyer - MTV
M. L. Seccomb - MAP
W. H. Shirey - SL
A. T. Strickland - SL
M. J. Swetnick - SL
J. H. Turnock - MA-4
G. C. White, Jr. - MAR
NASA Hq. Library - ATSS-10

Manned Spacecraft Center

J. E. Dornbach - ET33 (3)
J. H. Sasser - ET33

Marshall Space Flight Center

J. Bensko - R-RP-J
J. A. Downey - R-RP-J
E. Stuhlinger - R-RP

Ames Research Center

D. E. Gault

Boeing Aircraft Company

J. M. Saari
R. W. Shorthill

Jet Propulsion Laboratory

L. D. Jaffe - 351

Langley Research Center

N. L. Crabill - 159
C. H. Nelson - 159
A. T. Young - 159

U.S. Geological Survey (Flagstaff)

L. Rowan
E. M. Shoemaker
K. Watson

U.S. Geological Survey (Menlo Park)

H. Masursky

Bellcomm, Inc.

G. M. Anderson
J. P. Downs
R. E. Gradle
D. R. Hagner
P. L. Havenstein
W. C. Hittinger
B. T. Howard
D. B. James
C. A. Lovell
K. E. Martersteck
R. K. McFarland
J. Z. Menard
I. D. Nehama
G. T. Orrok
I. M. Ross
C. M. Thomas
T. H. Thompson
W. B. Thompson
C. C. Tiffany
J. M. Tschirgi
R. L. Wagner
All members, Division 101
Department 1023
Library
Central File